Published in final edited form as:

Laryngoscope. 2020 September ; 130(9): 2138–2143. doi:10.1002/lary.28400.

Peak sinus pressures during sneezing in healthy controls and post-skull base surgery patients

Zhenxing Wu, PhD[1], **John R Craig, MD**[2], **Guillermo Maza, MD**[1,3], **Chengyu Li, PhD**[1,4], **Bradley A Otto, MD**[1], **Alexander A Farag, MD**[1], **Ricardo L. Carrau, MD, FACS**[1], **Kai Zhao, PhD**[1]

[1]Department of Otolaryngology - Head & Neck Surgery, the Ohio State University, Columbus, OH

[2]Department of Otolaryngology, Henry Ford Health System, Detroit, MI

[3]Current: Department of Otolaryngology – Head & Neck Surgery, Southern Illinois University, Springfield IL

[4]Current: Department of Mechanical Engineering, Villanova University, Villanova, PA

Abstract

Objective: Patients are frequently advised to sneeze with an open mouth and avoid nose-blowing following endoscopic endonasal approaches (EEA) to skull base, despite a lack of quantitative evidence. This study applies computational fluid dynamics (CFD) to quantify sinus pressures along the skull base during sneezing.

Methods: CT or MRI scans of four post-EEA patients and four healthy controls were collected and analyzed utilizing CFD techniques. A pressure drop of 6000Pa was applied to the nasopharynx based on values in literature to simulate expiratory nasal airflow during sneezing. Peak pressures along the skull base in frontal, ethmoid and sphenoid sinuses were collected.

Results: Significant increases in skull base peak pressure was observed during sneezing, with significant individual variations from 2185-5685 Pa. Interestingly, healthy controls had significantly higher pressures compared to post-EEA patients (5179.37±198.42 Pa versus patients 3347.82±1472.20 Pa, $p<0.05$), which could be related to higher anterior nasal resistance in unoperated healthy controls (0.44±0.22 versus patients 0.31±0.16 Pa/ml/s, $p=0.38$). The sinus pressure build-up may be due to airway resistance functioning as a valve preventing air from being released quickly. Supporting this theory, there was a strong correlation ($r=0.82$) between peak skull base pressure and the ratio of anterior resistance to total resistance. Within-subject variation in pressures between different skull base regions was much lower (average~5%).

Conclusion: This study provided the first quantitative analysis of air pressure along the skull base during sneezing in post-EEA patients through CFD, suggesting the pressure build-up may depend on individual anatomy.

Corresponding Author: Kai Zhao, Ph.D, Associate Professor, Department of Otolaryngology - Head & Neck Surgery, The Ohio State University, 915 Olentangy River Rd., Office 4235, Columbus, OH 43212, 614-293-3857 (office); 614-366-1794 (lab); 614-293-7476 (fax), zhao.1949@osu.edu; kai.zhao@osumc.edu.

Level of Evidence: 3b

The authors have no financial interest and conflict of interest to disclose.

Keywords

Skull base surgery; computational fluid dynamics; nasal airflow dynamics

INTRODUCTION

Endoscopic endonasal approaches (EEAs) refer to transnasal surgical approaches to diagnose and resect intracranial tumors or other lesions involving the skull base [1-4]. The sinonasal cavities can be opened to create wide corridors to different areas of the skull base necessary for treatment of given skull base pathology. To achieve this transnasal access, the middle and superior turbinates, and nasal septum may require removal, and a variable number of sinus cavities may require opening. Performing these maneuvers not only leaves a large wound surface area at risk for postoperative hemorrhage, but the skull base surgery itself requires an opening be created between the sinus and intracranial cavities which is at risk for postoperative cerebrospinal fluid leakage or pneumocephalus should the skull base reconstruction fail. Based largely on intuition and expert opinion, certain precautions are recommended postoperatively to decrease intravascular, intranasal, and intracranial pressure spikes, so as to decrease the risks of the aforementioned complications[5]. For example, patients are generally advised to avoiding nose blowing, and to sneeze or cough with an open mouth, presumably decreasing the risk of high pressures being transmitted to vasculature, intranasal/sinus, and intracranial spaces[6] which could otherwise cause epistaxis or dislodging of one or more layers of the skull base reconstruction. However, methodical evaluation of the effects of these actions has not been conducted. For example, it is known that sneezing through the nose will generate high intranasal air pressure[7,8], but exactly how much of that pressure is transferred to the paranasal sinuses and skull base is unknown.

In the present study, a computational fluid dynamics (CFD) method[9] was applied to simulate airflow and pressure distribution inside the nasal and sinus cavities during sneezing, and to quantify the skull base sinus pressures among both post-EEA patients and healthy controls. Differences in pressure changes between the post-EEA patients and healthy controls during sneezing will be shown, and the potential impact of different flow properties, such as the flow resistance and flow rate, on the pressure will be discussed.

MATERIALS AND METHODS

Subjects

Four post-EEA patients (2 males, 2 females) were enrolled from a previous study[10]. Their ages ranged from 40-56 years (Table 1). These EEA patients were treated during the past 5 years at The Ohio State University (OSU) Wexner Medical Center and underwent postoperative high-resolution sinus computed tomography (CT) or magnetic resonance imaging (MRI) scans (Fig. 1). Patient 1 underwent an endoscopic endonasal transpterygoid approach for resection of left middle cranial fossa encephalocele, which included a left maxillary antrostomy, partial ethmoidectomy, and partial superior turbinectomy. Patient 2 underwent an endoscopic transsellar/tuberculum/planum approach to resect an optic canal meningioma, which also included a right maxillary antrostomy and total ethmoidectomy,

and left anterior ethmoidectomy. Both patients 3 and 4 underwent transsphenoidal approaches to resect pituitary adenomas, as well as bilateral submucosal inferior turbinate reductions, right maxillary antrostomy, total ethmoidectomy and superior turbinectomy. Patient 3 also had a left total ethmoidectomy and superior turbinectomy. All patients also underwent wide sphenoidotomies, posterior septectomies (with resection more caudally in patients 1 and 2). No patient presented with a preoperative history of prior radiotherapy, chronic rhinosinusitis, or nasal obstruction.

Four gender matched healthy controls were randomly selected also from previous studies[11-13]. Their ages ranged from 23-39 years (median, 32 years), and they had no preexisting nasal conditions or previous sinonasal surgery. The study was approved by the Institutional Review Board of the Ohio State University.

Computational method

Computational fluid dynamics (CFD) method was applied to simulate expiratory nasal airflow during sneezing and quantified the sinus pressures along the skull base. The general procedures of nasal CFD modeling were widely described in previous literature[10-21]. In brief here, the commercial software AMIRA (Visualization Sciences Group, Hillsboro, OR) was used to create the 3-D models of the nasal cavity based on the CT and MRI scans for each subject. Then tetrahedron element meshes with boundary prism layers were generated using the commercial software ICEM CFD (Ansys, Inc, Canonsburg, PA). The final meshes used to simulate the nasal cavity for each subject ranged from 1.6 to 3.6 million hybrid finite elements. The commercial CFD software ANSYS Fluent 19.2 was employed to calculate the momentum and pressure distribution of sneezing process inside the nasal cavity. A total pressure of 6000 Pa was applied to the nasopharynx of all subjects based on data in literature[7,8] to simulate the pressure force during human sneezing and the atmospheric pressure (0 Pa) was considered at the nostrils. The k-ω model was applied to solve the turbulent flow in our model. The SIMPLEC algorithm and second-order upwind scheme were used for the numerical simulations. The converged simulation results were determined once the residual of each variable was less than 10^{-5}. The numerical methods and meshing protocol applied in this study has been previously validated against experimental measurements[20]. Both steady state and transient simulations were carried out, and no obvious differences were found between them. The results shown in present study were based on steady state simulation.

Data Analysis

For each model, we separated the skull base area into three sections, as shown in Figure 2A, front, middle, posterior sections. The front section covered mostly the frontal sinus, the posterior section covered the sphenoid sinus, and the middle section covered what was in between, mostly the ethmoid sinuses. The maximum pressure values were reported within these skull base sections. Statistical comparison of the skull base peak pressure in these sections between patients and healthy controls was analyzed using independent two-tailed t tests as shown in Table 1 and Figure 2C. A modified power analysis (developed by Erdfelder)[22,23] specifically for small sample was applied to ensure that sufficient Power (1-β) of 80% were achieved.

RESULTS

Pressure distribution along skull base

During sneezing, peak pressures along the three skull base regions were significantly higher compared to reported pressure drops during normal resting breathing (15 Pa from nares to nasopharynx)[11,24]. This is in part, due to the large pressure drop applied during sneezing (6000 Pa)[7,8]. However, not all 6000 Pa of pressure was transferred to the skull base, with peak skull base pressures varying significantly between individuals, from 2185-5685 Pa (see Table 1). Interestingly, healthy controls had significantly higher peak pressures compared to EEA patients during sneezing (see Figure 2C: average peak pressure at all three sections of skull base of healthy controls were 5179.37 ± 198.42 Pa versus 3347.82 ± 1472.20 Pa in EEA patients, $p<0.05$ and power >80%). Figure 3 also shows that within each subject, pressure distributed quite evenly along all regions of the skull base, regardless of being patient or healthy control. The peak pressures at front, middle, and posterior skull base regions for every subject were summarized in Table 1. Within each subject, the variation in peak pressure values between the three skull base regions was minimal (average~5%).

Resistance in anterior nasal airway

By examining the pressure plots of healthy controls versus EEA patients, healthy controls were found to have higher pressure gradients in the anterior nasal airway (near nasal valve region). To explore the relationship between the peak pressure and this pressure gradients, regional pressure drop and nasal resistance in this anterior section (as shown in Figure 2B) were calculated for all the EEA patients and healthy controls. As can be found in Table 1, the healthy controls had higher anterior nasal pressure drops compared to post-EEA patients (3153.22 ± 957.36 Pa versus EEA patients 1601.83 ± 1087.70 Pa, $p=0.077$). Therefore, healthy controls also had higher anterior nasal resistance than EEA patients (0.44 ± 0.22 versus patients 0.31 ± 0.16 Pa/ml/s, $p=0.38$). To evaluate the impact of nasal resistance on the skull base pressure distribution, we examined the correlation between the peak skull base pressure and the ratio of the anterior nasal resistance to the total nasal resistance, and a strong correlation ($r=0.82$) was found as shown in Figure 2D.

DISCUSSION

EEA has gradually replaced traditional open approaches for accessing skull base pathology, and repair of the resultant skull base defects and cerebrospinal fluid leaks has dramatically improved over the years. EEA requires variable degrees of sinus opening, and often requires resection of the middle and superior, possibly inferior turbinates, and nasal septum. The postoperative wound after EEA includes exposed bone and submucosal vasculature of the sinus cavities, and the skull base reconstruction site which often includes a multilayer reconstruction with various intracranial grafts and likely a mucosal onlay/overlay graft on the sinus side of the skull base defect. Therefore there are concerns postoperatively with significant pressure changes in the vascular, sinonasal, and intracranial spaces, which could lead to previously mentioned complications (epistaxis and failure of the CSF leak repair with resultant pneumocephalus or meningitis)[5]. Patients are frequently advised postoperatively after EEA to avoid straining and nose blowing, and to sneeze and cough

through an open mouth to prevent significant pressure spikes and aforementioned complications. However, evidence behind these recommendations for postoperative precautions has been limited.

In the current study, airflow was simulated inside human nasal cavities during sneezing through the nose using CFD modeling. Compared to the normal resting breathing pressure drop from the nares to nasopharynx (15 Pa)[11,24], peak pressures along the skull base section were significantly higher during a sneeze, which was likely due to the enormous high pressure exerted by the subjects during sneeze (~6000 Pa)[7,8]. However, only a portion of that 6000 Pa pressure is transferred to the skull base. Healthy controls surprisingly generated significantly higher mean peak pressures at the skull base than EEA patients during sneezing (5179.37 ± 198.42 Pa in healthy controls versus 3347.82 ± 1472.20 Pa in EEA patients, $p<0.05$). Although no human data is available on the clinical consequences of these pressure values, limited animal data do exist measuring burst pressures - pressure at which various tissue flap or skull base repair failed. For example, burst pressures ranged from 1125 Pa to 4650 Pa (converted from mmHg) for a single layer of sheep septal mucosa or periosteum flap with various incision, after sutured and laser welded.[25] However, an intact septal mucosa flap and periosteum did not fail at the maximum experimental pressure of 103458 Pascal. An averaged burst pressure ranged from 31716 Pa to 95148 Pa in pig skull base repaired with different techniques[26]. In comparison, the current study's model predicted peak pressures in the range of the burst pressure of single layer tissue grafts/flaps with suture/wield, but were far below the burst pressure of intact tissue flaps and skull base repairs. These comparisons may be helpful for future clinical insight.

One possible explanation for the higher peak pressure in healthy controls could be their higher anterior nasal resistances (0.44 ± 0.22 Pa/ml/s) compared to EEA patients (0.31±0.16 Pa/ml/s). In skull base approaches, most surgeries were also performed to the patient's anterior half of the nasal airway, including inferior and middle turbinates and nasal septal resection. The anterior nasal cavity has been known to contribute importantly to overall nasal resistance. The pressure accumulation seen in the sinuses and along skull base in both the healthy controls and EEA patients could be due to nasal resistance preventing air from being released quickly from the nasal cavity, like a valve. The EEA patients could have had the anterior half of the nasal cavity opened more than the healthy controls, which led to lower resistance in the anterior nasal cavity, and lower peak pressure along the skull base. In support of this theory, a significant amount of the anterior septum was removed in patients 1 and 2, and the inferior turbinates were significantly reduced in patient 3, so these operative maneuvers could have resulted in decreased resistance in the anterior half of the nasal cavities. For EEA patient 4, the septum and inferior turbinates were not resected or significantly reduced, and this patient had the highest anterior nasal resistance (0.55 Pa/ml/s) and corresponding highest peak skull based pressure among all patients as shown in Table 1. Patient 4's anterior nasal resistance was more similar to healthy controls which led to a sinonasal pressure distribution more similar to healthy controls as shown in Figure 3H. The strong correlation between the peak skull base pressure and the ratio of anterior nasal resistance to nasal total resistance ($r=0.82$) gave support to the theory that nasal resistance changes could account for the differences seen between EEA patients and controls. It should be noted that the nasopharynx could potentially be a significant contributor to the total

resistance in some subjects or patients, depending on the individual shape of the nasopharynx. But this is likely a pre-existing factor not affected by EEA surgery. In our current study, we tried to truncate each model consistently in the nasopharynx region above the soft palate to minimize this confounding factor.

Another interesting finding from the current study was that the pressure values were pretty uniform across each of the measured points along the skull base within each subjects for both the healthy controls and EEA patients (average~5%, see Table 1 and Figure 3), despite the significant peak pressure variations between the subjects (from 2185-5685 Pa). One possible explanation for these findings could be that the skull base is connected to the middle region of sinonasal cavity that has a relatively large cross-sectional areas and low regional nasal resistance, which could lead to a small within-subject pressure gradient in this region. The low within-subject resistance variations of the middle nasal region may lead to the low pressure variations along the skull base regions, within subjects. On the other hand, the larger between-subject variations in anterior nasal resistance may lead to the larger between-subjection variations in peak skull base pressure.

The main limitations of the study included the small sample size and the heterogeneous surgical approaches among the patients. However, we did find statistical significance in some of our analysis with sufficient power ($1-\beta > 80\%$)[22,23] in this preliminary study, despite the small size. Larger studies will need to be performed in the future. Secondly, the CFD modeling also revealed that the different surgical approaches to the sinuses and skull base may have a limited effect on the skull base pressure differences. For example, even healthy controls with unoperated sinuses had quite uniform and higher pressure distribution along the skull base than patients – so surgeries do not necessarily expose the skull base to more pressure. However, the extent of surgery in the anterior half of the nasal airway, as well as anatomical variations in anterior or posterior nasal airway resistance, did have an impact on the skull base pressure build-up. This study could promote an interest in studying the utility of postoperative nasal precautions in the setting of skull base surgery, and specifically whether patients and surgeons need to worry about sneezing pressures.

CONCLUSION

This study provided the first quantitative analysis of air pressure along the skull base during sneezing through the nasal airway in post-EEA patients through CFD, and reported significant individual variations in skull base pressure depending on individual anatomy differences, but also uniform distribution of those pressures across all skull base regions.

Acknowledgments

This research was supported by NIH NIDCD R01 DC013626 to KZ.

BIBLIOGRAPHY

1. Cappabianca P, Cavallo LM, Esposito F, de Divitiis O, Messina A, de Divitiis E. Extended endoscopic endonasal approach to the midline skull base: the evolving role of transsphenoidal surgery In: Pickard JD, Akalan N, Di Rocco C, et al., eds. Advances and Technical Standards in Neurosurgery. Vienna: Springer Vienna; 2008:151–199. doi:10.1007/978-3-211-72283-1_4

2. Cavallo LM, Messina A, Cappabianca P, et al. Endoscopic endonasal surgery of the midline skull base: anatomical study and clinical considerations. Neurosurg Focus. 2005;19(1):1–14. doi:10.3171/foc.2005.19.1.3

3. Kassam A, Snyderman CH, Mintz A, Gardner P, Carrau RL. Expanded endonasal approach: the rostrocaudal axis. Part II. Posterior clinoids to the foramen magnum. Neurosurg Focus. 2005;19(1):1–7. doi:10.3171/foc.2005.19.1.5

4. Kassam A, Snyderman CH, Mintz A, Gardner P, Carrau RL. Expanded endonasal approach: the rostrocaudal axis. Part I. Crista galli to the sella turcica. Neurosurg Focus. 2005;19(1):1–12. doi:10.3171/foc.2005.19.1.4

5. Horowitz PM, DiNapoli V, Su SY, Raza SM. Complication Avoidance in Endoscopic Skull Base Surgery. Otolaryngol Clin North Am. 2016;49(1):227–235. doi:10.1016/j.otc.2015.09.014 [PubMed: 26614840]

6. Phillips N, Nix P. How I do it - endoscopic endonasal approach for pituitary tumour. Acta Neurochir (Wien). 2016;158(10):1983–1985. doi:10.1007/s00701-016-2916-z [PubMed: 27526186]

7. Rahiminejad M, Haghighi A, Dastan A, Abouali O, Farid M, Ahmadi G. Computer simulations of pressure and velocity fields in a human upper airway during sneezing. Comput Biol Med. 2016;71:115–127. doi:10.1016/j.compbiomed.2016.01.022 [PubMed: 26914240]

8. Lausted CG, Johnson AT, Scott WH, Johnson MM, Coyne KM, Coursey DC. Maximum static inspiratory and expiratory pressures with different lung volumes. Biomed Eng OnLine. 2006;5(1):29. doi:10.1186/1475-925X-5-29 [PubMed: 16677384]

9. Subramaniam RaviP, Richardson ReginaB, Morgan KevinT, Kimbell JuliaS, Guilmette RaymondA. COMPUTATIONAL FLUID DYNAMICS SIMULATIONS OF INSPIRATORY AIRFLOW IN THE HUMAN NOSE AND NASOPHARYNX. Inhal Toxicol. 1998;10(2):91–120. doi:10.1080/089583798197772

10. Maza G, Li C, Krebs JP, et al. Computational fluid dynamics after endoscopic endonasal skull base surgery-possible empty nose syndrome in the context of middle turbinate resection: Endoscopic skull base surgery and ENS-a CFD study. Int Forum Allergy Rhinol. 2019;9(2):204–211. doi:10.1002/alr.22236 [PubMed: 30488577]

11. Zhao K, Jiang J. What is normal nasal airflow? A computational study of 22 healthy adults: Normal human nasal airflow. Int Forum Allergy Rhinol. 2014;4(6):435–446. doi:10.1002/alr.21319 [PubMed: 24664528]

12. Li C, Farag AA, Maza G, et al. Investigation of the abnormal nasal aerodynamics and trigeminal functions among empty nose syndrome patients: Abnormal nasal aerodynamics in ENS patients. Int Forum Allergy Rhinol. 2018;8(3):444–452. doi:10.1002/alr.22045 [PubMed: 29165896]

13. Zhao K, Jiang J, Blacker K, et al. Regional peak mucosal cooling predicts the perception of nasal patency: Mucosal Cooling and Nasal Patency. The Laryngoscope. 2014;124(3):589–595. doi:10.1002/lary.24265 [PubMed: 23775640]

14. Zhao K Effect of Anatomy on Human Nasal Air Flow and Odorant Transport Patterns: Implications for Olfaction. Chem Senses. 2004;29(5):365–379. doi:10.1093/chemse/bjh033 [PubMed: 15201204]

15. Li C, Farag AA, Leach J, et al. Computational fluid dynamics and trigeminal sensory examinations of empty nose syndrome patients: Computational and Trigeminal Studies of ENS. The Laryngoscope. 2017;127(6):E176–E184. doi:10.1002/lary.26530 [PubMed: 28278356]

16. Otto BA, Li C, Farag AA, et al. Computational fluid dynamics evaluation of posterior septectomy as a viable treatment option for large septal perforations: CFD analysis of nasal septal perforation. Int Forum Allergy Rhinol. 2017;7(7):718–725. doi:10.1002/alr.21951 [PubMed: 28544511]

17. Lee TS, Goyal P, Li C, Zhao K. Computational Fluid Dynamics to Evaluate the Effectiveness of Inferior Turbinate Reduction Techniques to Improve Nasal Airflow. JAMA Facial Plast Surg. 2018;20(4):263. doi:10.1001/jamafacial.2017.2296 [PubMed: 29372235]

18. Shen J, Hur K, Zhao K, Leopold D, Wrobel B. Determinants and Evaluation of Nasal Airflow Perception. Facial Plast Surg. 2017;33(04):372–377. doi:10.1055/s-0037-1603788 [PubMed: 28753710]

19. Li C, Jiang J, Kim K, et al. Nasal Structural and Aerodynamic Features That May Benefit Normal Olfactory Sensitivity. Chem Senses. 2018;43(4):229–237. doi:10.1093/chemse/bjy013 [PubMed: 29474516]

20. Li C, Jiang J, Dong H, Zhao K. Computational modeling and validation of human nasal airflow under various breathing conditions. J Biomech. 2017;64:59–68. doi:10.1016/j.jbiomech.2017.08.031 [PubMed: 28893392]

21. Zhao K, Malhotra P, Rosen D, Dalton P, Pribitkin EA. Computational Fluid Dynamics as Surgical Planning Tool: A Pilot Study on Middle Turbinate Resection: CFD AND NASAL SURGERY. Anat Rec. 2014;297(11):2187–2195. doi:10.1002/ar.23033

22. Erdfelder E Zur Bedeutung und Kontrolle des !B-Fehlers bei der inferenzstatistischen Prüfung log-linearer Modelle. [The significance and control of the !B-error during the inference-statistical examination of the log-linear models.]. Z Für Sozialpsychologie. 1984;15(1):18–32.

23. Faul F, Erdfelder E, Lang A-G, Buchner A. G*Power 3: A flexible statistical power analysis program for the social, behavioral, and biomedical sciences. Behav Res Methods. 2007;39(2):175–191. doi:10.3758/BF03193146 [PubMed: 17695343]

24. Keyhani K, Scherer PW, Mozell MM. Numerical Simulation of Airflow in the Human Nasal Cavity. J Biomech Eng. 1995;117(4):429–441. doi:10.1115/1.2794204 [PubMed: 8748525]

25. Bleier BS, Palmer JN, Sparano AM, Cohen NA. Laser-assisted cerebrospinal fluid leak repair: An animal model to test feasibility. Otolaryngol Neck Surg. 2007;137(5):810–814. doi:10.1016/j.otohns.2007.05.060

26. de Almeida JR, Ghotme K, Leong I, Drake J, James AL, Witterick IJ. A New Porcine Skull Base Model: Fibrin Glue Improves Strength of Cerebrospinal Fluid leak Repairs. Otolaryngol Neck Surg. 2009;141(2):184–189. doi:10.1016/j.otohns.2009.03.008

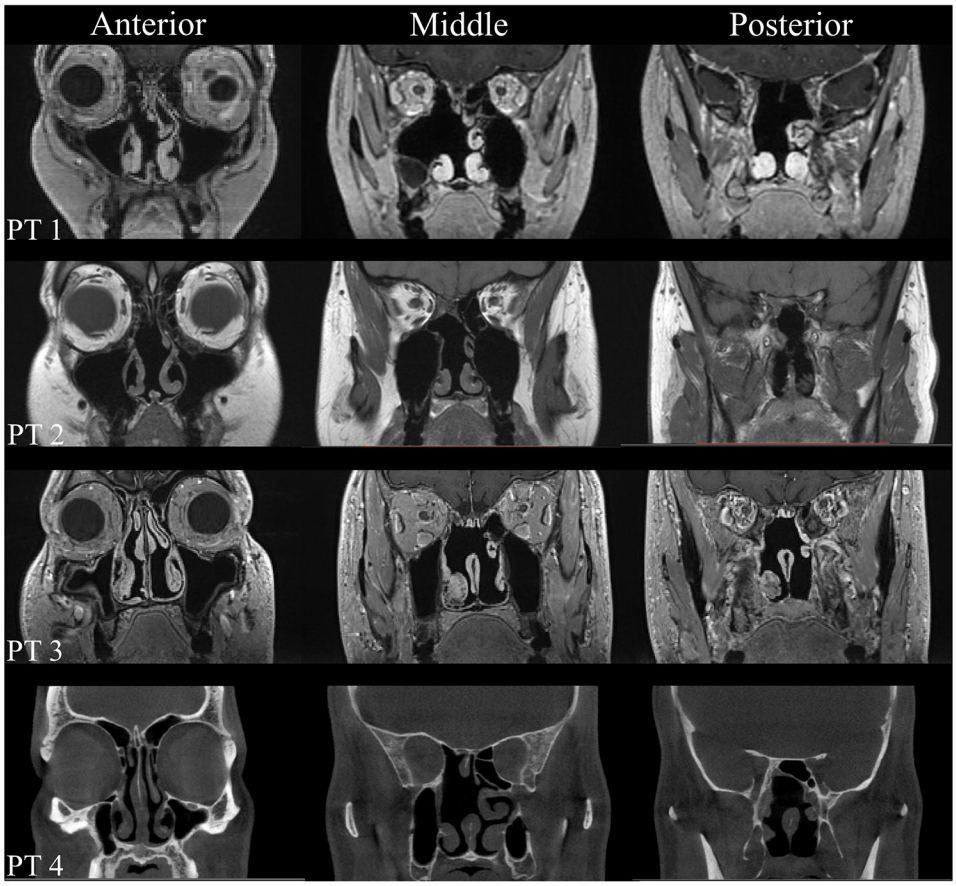

Figure 1.

Coronal MRIs of the paranasal sinuses in EEA patients. Patient 1 (PT 1), Patient 2 (PT 2) and Patient 3 (PT3): coronal T1-weighted MRIs anteriorly, middle, and posteriorly; Patient 4 (PT 4): coronal head CT anteriorly, middle, and posteriorly. CT = computed tomography; MRI = magnetic resonance imaging.

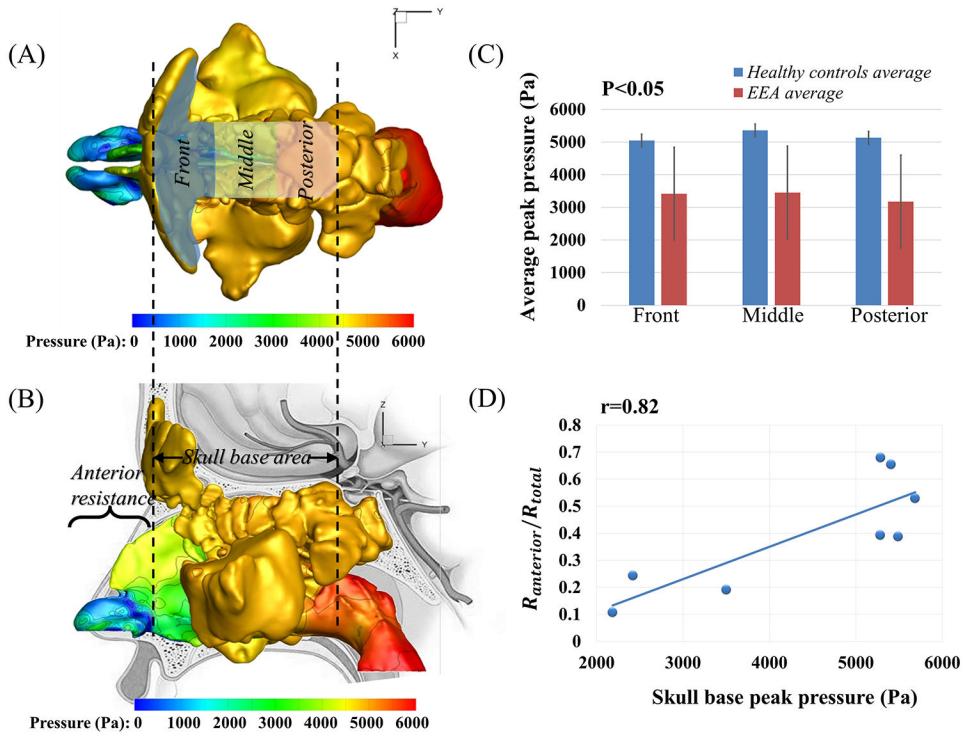

Figure 2.

(A) The top view of the pressure distribution (Pascal) in the nasal cavity of healthy control 1. The skull base area was further divided into front, middle, and posterior sections; (B) The lateral view of the pressure distribution in the nasal cavity of healthy control 1, with the indication of the anterior nasal resistance; (C) The comparison of the peak pressure at different skull base sections between healthy controls and EEA patients; (D) The Pearson correlation between the skull base peak pressure and the ratio of anterior resistance to total resistance for all the healthy controls and EEA patients.

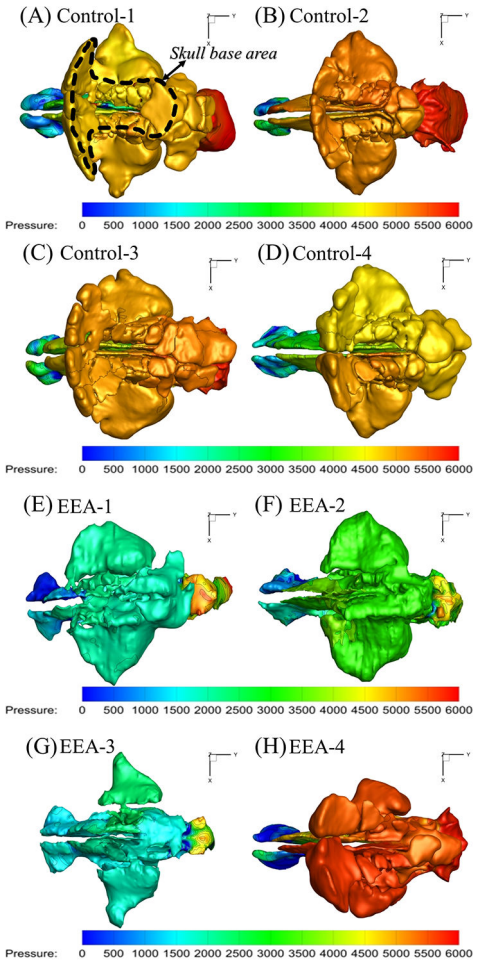

Figure 3.

Top view of pressure (Pascal) distribution in sinonasal cavities of four healthy controls, (A)-(D) and 4 EEA patients (E)-(H).

Table 1.

Summary of demographics and results

Subject #	EEA#1	EEA#2	EEA#3	EEA#4	Control#1	Control#2	Control#3	Control#4
Gender	F	F	M	M	M	F	F	M
Age (years)	56	52	56	40	39	27	23	37
FU (months)	26	15	60	36	N/A	N/A	N/A	N/A
FPP (Pa)	2146.8	3484.6	2385.3	5661.5	4816.7	5214.8	5126.7	5026.5
MPP (Pa)	2185.3	3498.6	2421.7	5685.0	5488.9	5405.3	5262.0	5282.9
PPP (Pa)	1968.4	3430.1	1877.0	5429.5	4982.3	5295.4	5286.1	4964.8
SBPP (Pa)	2185.3	3498.6	2421.7	5685.0	5489	5405.3	5286.1	5282.9
Variation	5.5%	1.0%	13.7%	2.5%	6.9%	1.8%	1.6%	3.3%
Flowrate (m^3/s)	0.0034	0.0048	0.0052	0.0058	0.0090	0.0057	0.0072	0.0091
APD (Pa)	639	1145	1473	3150	2301	3908	4053	2351
AR (Pa/ml/s)	0.19	0.24	0.28	0.55	0.26	0.69	0.57	0.26

APD= anterior pressure-drop; AR= anterior Resistance; FPP= front peak pressure; FU= follow-up time; MPP= middle peak pressure; PPP= posterior peak pressure; SBPP= skull base peak pressure.